

## Optimization of Thermal Performance of a Segmental Baffle Shell and Tube Heat Exchanger under Different Baffle Spaces and Baffle Numbers: A Numerical Case Study Using CFD

*Md. Tofazzal Hossain<sup>1,\*</sup>, Badhan Saha<sup>2</sup>*

*<sup>1,2</sup>Department of Mechanical and Production Engineering, Ahsanullah University of Science and Technology, Dhaka 1208, Bangladesh*

*\*Corresponding Author*

*E-mail Id:-tofazzal.me@aust.edu*

### ABSTRACT

*In the fields of engineering, heat exchanger devices play an important role in multipurpose thermal engineering processes related to power generation and transformation of energy in the industrial arena. Nowadays, the optimization of the design and modeling of a shell and tube heat exchanger has become an engineering challenge. In this paper, a shell and tube heat exchanger with segmental baffles and hexagonal arrangement of 19 tubes have been designed and studied with the help of the commercial software package ANSYS FLUENT 18.1. Numerous attempts have been performed to seek out the effects of baffle spaces and baffle numbers on the heat transfer and the patterns of streamlines of fluid flow with similar geometrical configurations and boundary conditions. The designed baffle spaces and baffle numbers are: for case A: 80 mm with 6 baffle numbers, for case B: 100 mm with 5 baffle numbers, for case C: 125 mm with 4 baffle numbers, and for case D: 150 mm with 4 baffle numbers. The results of this study indicate the highest heat transfer coefficients, and highest turbulence intensity, less viscous intensity, and most uniform temperature distributions occur in case B. However, an appropriate combination of baffle spaces and baffle numbers is highly recommended to acquire the significant amount of heat transfer and temperature variations.*

**Keywords:-***Baffle numbers, baffle spaces, heat exchanger, heat transfer, segmental baffles*

### INTRODUCTION

In the fields of engineering, heat exchanger devices play an important role in multipurpose thermal engineering processes, for example, petrochemical and oil industries, food industry, electric power generation, etc. [1-3]. There are numerous types of heat exchangers available in engineering applications, such as parallel (unidirectional) flow heat exchanger, counter (reciprocal) flow heat exchanger, shell and tube heat exchanger (STHX) and cross (mixed) flow heat exchanger. On the basis of heat exchanger analysis methods, for instance, log mean temperature difference (LMTD), and effectiveness-NTU methods, STHXs are the most appropriate

selection to facilitate the rate of heat transfer [4]. The multipurpose thermal engineering application prospects rendered by the STHXs make this an integral part of playing a fundamental role in these industrial outgrowths. To rationalize the consumption of energy in the field of thermal engineering, performance enhancement is considered as a prime factor [1]. The heat flux is a strong function of the pattern of flow and the flow patterns depend on the several geometrical parameters of the STHXs. Most of the research has been performed to modify the design of STHXs and flow patterns to improve the heat transfer rates [1]. Various types of baffles are used in STHXs to

facilitate the flow patterns for optimizing the heat transfer rate within the same inlet and outlet temperatures, and same mass flow rate. The relative position, orientation, number of baffles, the distance between the adjacent baffles, shape, and size of the baffles, the position of the two extreme end baffles i.e. inlet and outlet section baffles, and the percentage of clearance space between baffle and shell are the essential factors to accelerate the thermal performance with the improved turbulence effects of the shell side fluid flow and to gain a better heat transfer coefficient. The triangular, rectangular, square, circular, and hexagonal arrangements of the tubes are also vital factors to enrich the heat transfer rate. Moreover, the number of tube passes and shell passes are important design criteria in favor of enriched heat transfer within a small volume [4].

M. Mellal et al. [1] sought out a 3D numerical study using CFD COMSOL Multiphysics 5.1 software to investigate the effects of turbulence of fluid flow as well as the heat transfer in an STHX. They have performed their study with the modification of baffle spaces and baffles orientation angles. The validation of their results has been done with the available experimental data and concluded that for the baffle space of 64 mm and orientation angle of  $180^\circ$  are the best design criteria to obtain the maximum value of thermal performance in comparison to the STHX without baffles. Experimental and numerical investigations have been carried out by J. Wen et al. [5] to investigate the performance of the STHX with different baffles. From their observations, they have found that the ladder-type arrangement of baffles is the most effective design parameter to excel the heat transfer performance of the STHXs with helical baffles. They have culminated their outcomes that the convective heat transfer coefficient in the shell side fluid and the overall coefficient of heat transfer have been improved by 22.3–32.6 % and 18.1–22.5 %, respectively with this special

type of baffle arrangement. The pumping power varies within 2 to 80 W with the increment of pressure drop of about 0.911–9.084 kPa. Houari Ameer [6] performed a numerical simulation to estimate the heat transfer performance in a channel-type heat exchanging device with the inclusions of corrugated baffle arrangements. The author has done the study with the insertion of wavy type corrugated baffles by changing the angle of baffles from  $0^\circ$  (flat baffle) to  $45^\circ$ . In his research, the author has considered three different ratios of the height of the baffles and channel to optimize the thermal performance of the heat exchanger. The overall performance factor has increased from 1.27 to 1.53 with the variation of corrugation angle from  $0^\circ$  to  $45^\circ$  and obtained the best results of thermal performance for the ratio of baffle height to the channel of 0.5. M.H. Mohammadi, et al. [7] have been performed a numerical study to optimize the heat transfer performance of an STHX using porous baffles. The authors have investigated the rate of heat transfer and pressure gradient along the STHX. In their study, the authors have used 6 porous baffles in three different substructures such as porosity, permeability, and the percentages of baffle cut to investigate the effects of the segmental porous baffles. They have found that the pressure drop and the heat transfer were increased while the baffle cut was decreased. The authors concluded in their investigation that lower baffle cut behaves as the obstacle to optimize the heat transfer rate as the pressure drop becomes higher. The authors have overcome this obstacle to optimize the heat transfer with a call upon the combination of porosity, permeability, and the percentages of baffle cut using the genetic algorithm (GA) method. A three-dimensional CFD analysis was performed by S. Gaikwad and A. Parmar [8] to study the impact of baffle spacing and baffle cut by using commercial software ANSYS CFX. This study aimed to find an optimum

combination of baffle spacing and baffle cut for the efficacious performance of STHX. They have found that for a specific baffle cut, the heat transfer coefficient becomes higher with the higher number of baffles. Moreover, the pressure drop rises with the larger baffle spacing, which can be optimized by controlling the baffle cut. Kumaresan et al. [9] have investigated a numerical analysis on STHX performance with inclined baffles and the percentage of baffle cuts. The authors have considered several arrangements of baffle cuts and baffle inclination angle in this analysis, and found significant fluctuations in both the pressure drop as well as the rate of heat transfer across the STHX. The major finding of their study is that the heat transfer rate becomes maximum and the pressure drop becomes minimum for the inclination angle of baffles of  $35^\circ$  and the percentage of baffle cut of 30% of the shell inner diameter.

Li He and Peng Li [10] have done a computer simulation study on a single pass shell and double tube heat exchanger for different baffle configurations. They have explored the rate of heat transfer to optimize the power consumption using three different arrangements of baffles (helical baffles, segmental baffles, and flower baffles). They have found the highest heat transfer rate per effective pumping power for the flower baffle arrangement and the lowest heat transfer rate per effective pumping power for segmental baffle configuration. E. Kayabasi et al. [11] have investigated a numerical and experimental study on the effects of geometrical component dimensions such as, baffle cut, baffle spacing, the gap between heat exchanger components, sealing strips, and the number of tube and tube passes on pressure loss and heat transfer in STHX. They have utilized the HTRI Xchanger Suite Educational software for numerical analysis. They have achieved the highest heat transfer coefficient per unit pressure loss for the case of baffle spacing

and baffle cut of 60% and 25% of shell inner diameter respectively. The effects of the diametrical clearance between the sealing strips and the shell components have also been studied in this research. They have analyzed that higher pressure loss has been obtained when the baffle spacing and the number of tubes are minimum. Abbasi et al. [12] have performed a numerical study on shape optimization of porous baffles to enhance the thermal performance of STHX. In their study, three different geometrical parameters such as angle, thickness, and the number of baffles have been used. They have found that a higher number of baffles in the shell increase the heat transfer rate and the pressure drop. A multi-objective optimization method has been conducted in this research to optimize the higher heat transfer rate and lower pressure drop. They have obtained a minimum pressure drop of 48.87 kPa on the shell side with a maximum heat transfer rate of 523.81 kW for the geometrical configurations of the number of baffles, baffle angles and baffle thickness of 10,  $111.9^\circ$ , and 16.69 mm, respectively.

In this research, we have performed a numerical computational fluid dynamics (CFD) analysis using commercial academic software ANSYS 18.1 [13] to optimize the coefficient of heat transfer, and pressure drop. As the higher pressure drop requires a higher power consumption, the fabrication and design of an STHX become much more costly. From the literature review, it is seen that the pressure drop and heat transfer are highly dependent on various geometrical configurations of the STHX especially the baffle cut, baffle space, number of baffles, and arrangement of the tubes. As the experimental study is too expensive to perform the above-mentioned geometrical configurations, it is more feasible to perform these studies using numerical simulation. In our research, we have focused our study to minimize power consumption by optimizing the temperature

distribution and heat transfer. For the optimization of the temperature distribution and the rate of heat transfer, we have modified our design to achieve an optimum baffle space with a specific baffle cut of 25% and hexagonal arrangements for the tubes.

### MATERIALS AND METHODS

As shown in Figure 1, the model that has been studied in this research is a single tube pass and single shell pass counter-flow heat exchanger having the configurations of hexagonal pitch arrangements with 20 tubes and a gross length of 600 mm. The hexagonal arrangement of tubes has been selected in this study to optimize the heat transfer. Two major parameters such as the number of baffles (4, 5, and 6) and baffle spacing (80 mm, 100 mm, 125 mm, and 150 mm) have been investigated. A 25% baffle cut has been considered for all cases. From the literature review, it has been seen

that 25% diametrical clearance between the baffle and the inner diameter of the shell provides better thermal performance with minimum turbulence effect and less pressure drop. The shell side fluid is taken as cold water with an inlet temperature of 293 K and tube side fluid is taken as hot water with an inlet temperature of 343 K. Gauge pressure of 0 Pa has been set in both outlets of hot and cold fluids. The heat loss by conduction between hot water and tube walls and between cold fluid and tube walls has been neglected to have a negligible tube thickness of 3 mm. Moreover, the tube wall temperature has been kept constant with 343 K. No-slip boundary conditions have been considered at the adjacent walls of the shell and tubes. The heat loss by conduction through the baffles is overcome by considering the thin-walls method. All the necessary geometrical parameters and properties of fluid have been tabulated in Table 1.

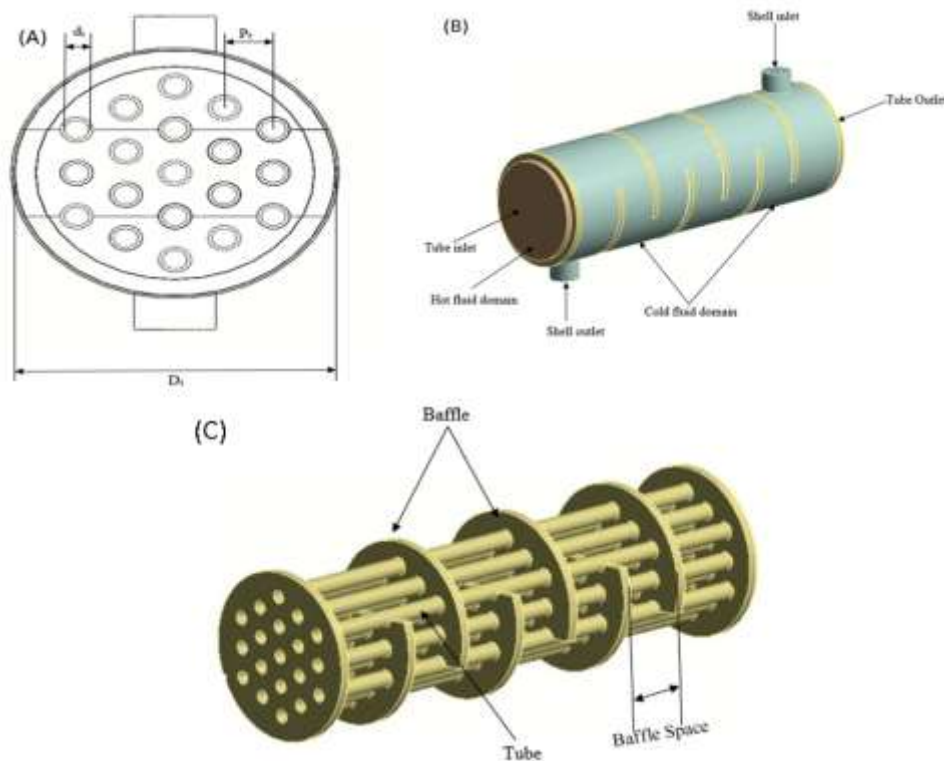


**Fig.1:-STHX arrangement with 6 baffles (A) Hexagonal tube arrangement (B) Fluid domains and boundaries (C) Baffle configurations**

**Table 1:-Geometrical parameters and boundary conditions.**

Items	Dimensions and Descriptions			
Cases	A	B	C	D
Shell Parameters:				
Total length, L (mm)	600	600	600	600
Inner diameter, D <sub>i</sub> (mm)	200	200	200	200
Thickness, t <sub>s</sub> (mm)	5	5	5	5
Tube Parameters:				
Inner Diameter, d <sub>i</sub> (mm)	20	20	20	20
Number	19	19	19	19
Thickness, t <sub>t</sub> (mm)	3	3	3	3
Pitch, P <sub>t</sub> (mm)	34.64	34.64	34.64	34.64
Arrangement	Hexagonal	Hexagonal	Hexagonal	Hexagonal
Baffle Parameters:				
Space, B (mm)	80	100	125	150
Number	6	5	4	4
Material	Copper	Copper	Copper	Copper
Thickness (mm)	5	5	5	5
Boundary Conditions				
Tube Inlet Temperature, T <sub>hot</sub> (K)			343	
Shell Inlet Temperature, T <sub>cold</sub> (K)			293	
Tube Inlet Mass Flow Rate, $\dot{m}_{hot}$ (kg/s)			2	
Shell Inlet Mass Flow Rate, $\dot{m}_{cold}$ (kg/s)			1.2	
Shell Wall Temperature, T <sub>shell</sub> (K)			293	

## MESH GENERATION

The investigated geometry as shown in Figure 2 was generated and meshed by using computer code ANSYS CFD version 18.1 [13]. The numerical analysis is strongly dependent on the proper grid system and structure. For complex geometry, it is best suited to utilize

tetrahedral grid elements [14] to mesh the computational domain. It is notable that the triangular shape grid elements generated by the Tet-Hybrid grid system are most appropriate to any complex geometry. Much finer mesh has developed at the different interface regions. To achieve better heat transfer



simulated results, it is highly desired to create appropriate mesh networks.

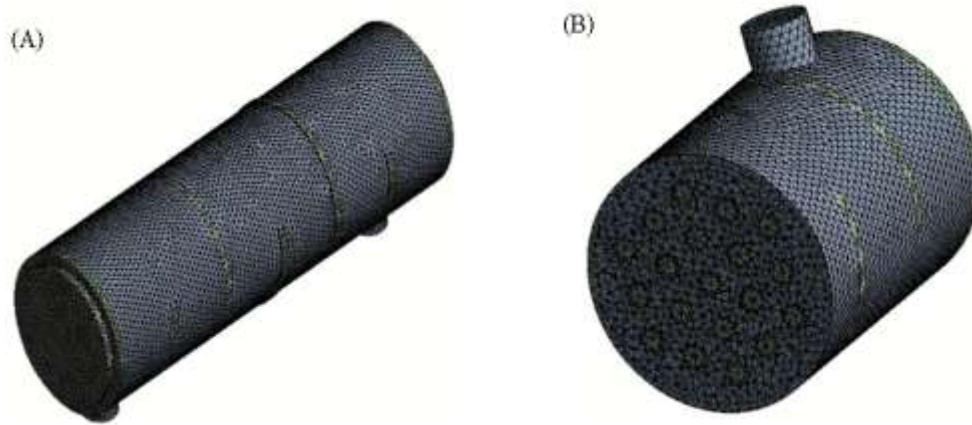


**Fig.2:-**Meshed geometry with tetrahedral grid elements: (A) 3-D geometry (B) half cross-sectional geometry

### MATHEMATICAL MODELING

The equations governed by the flow characteristics are utilized on the basis of the simulated conditions according to the peer concept of fluid dynamics and heat transfer principles. The compressibility of fluid flow is defined by the flow velocity relative to sound speed characterized by a non-dimensional parameter Mach number. For the stationary fluid flow models, an incompressible flow can be characterized by a low Mach number ( $\leq 0.3$ ) [4]. In this numerical simulation process, the renormalization group (RNG)  $k-\varepsilon$  turbulence model has been utilized for modeling the turbulent flow. The  $k-\varepsilon$

model is only applicable for the fully turbulent flows because it is assumed that the effects of the molecular viscosity are negligible and the flow is fully turbulent in the derivation of the  $k-\varepsilon$  model [13]. The RNG  $k-\varepsilon$  model requires less memory usage and shorter time for the calculation process comparing to the other available models. Moreover, this model is very important to predict the more accurate heat transfer output in the adjacent regions to the wall.

The mathematical modeling of energy, momentum, continuity,  $k$ , and  $\varepsilon$  in the CFD calculations are given bellows:

$$\text{Energy equation: } \rho c_p u (\nabla T) = \nabla \cdot (K \nabla T) + \phi \quad (1)$$

$$\text{Continuity equation: } \nabla \cdot (\rho u) = 0 \quad (2)$$

$$\text{Momentum equation: } (\nabla \cdot u) \rho u = -\nabla p + \nabla \cdot \mu (\nabla u + (\nabla u)^T) \quad (3)$$

The standard turbulence  $k-\varepsilon$  model is derived from the  $\varepsilon$  (energy dissipation) (Eq. (4)) and the  $k$  (turbulent kinetic energy) (Eq. (5)) has been utilized in this study.

$$\rho(u \cdot \nabla) \varepsilon = \nabla \cdot \left[ \left( \mu + \frac{\mu T}{\sigma \varepsilon} \right) \nabla \varepsilon \right] + C_{\varepsilon 1} \frac{\varepsilon}{k} P_k - C_{\varepsilon 1} \rho \frac{\varepsilon^2}{k}, \varepsilon = ep \quad (4)$$

$$\rho(u \cdot \nabla) k = \nabla \cdot \left[ \left( \mu + \frac{\mu T}{\sigma k} \right) \nabla k \right] + P_k - \rho \varepsilon \quad (5)$$

$$\text{where the production term is: } P_k = \mu_T [\nabla u : (\nabla u + (\nabla u)^T)] \quad (6)$$

The turbulent viscosity

is:

$$\mu_t = \rho C_\mu \frac{k^2}{\varepsilon} \quad (7)$$

The experimental constants for the standard turbulence k-ε model are given as follows:

$$C_{\varepsilon 1} = 1.44, C_{\varepsilon 2} = 1.92, C_\mu = 0.09, \sigma_k = 1, \sigma_\varepsilon = 1.3$$

Eq. 8 is used to calculate the friction factor (f) is coherently dependent on the pressure difference along the channel length (L) as,

$$f = \frac{2}{(L/D_h)} \frac{\Delta P}{\rho U^2} \quad (8)$$

The dimensionless local Nusselt number (Eq. 9) is used to find the convective heat transfer in comparison to conductive heat transfer within a layer of heat transfer.

$$Nu_{(x)} = \frac{h_x D_x}{K_F} \quad (9)$$

Total Nusselt number (Eq. 10) can be obtained by the area integral of Eq. 9

$$Nu = \frac{1}{A} \int Nu_{(x)} \partial A \quad (10)$$

The factor of thermal performance  $\eta$  is shown in Eq. 11

$$\eta = (Nu/Nu_0)/(f/f_0)^{1/3} \quad (11)$$

$f_0$  and  $Nu_0$  are the reference values of the base case (STHX with no baffles).

### TEST OF GRID INDEPENDENCE

The proper grid element system has a significant influence on the numerical analysis as well as the validation purpose. Therefore, to ensure the reliability of the numerical results, careful insights for grid independence are mandatory. To perform the independence test, 5 numbers of Tet-Hybrid grid element systems with different sizes have been taken into consideration. The number of grids has

been varied to corroborate the independence of the grids for the above-mentioned cases. The total heat transfer parameter is considered to facilitate the independence test. In this study, the grid sizes of 412890, 438582, 463765, and 508397 for cases A, B, C, and D, respectively have been adopted. The different grid sizes and corresponding heat transfer of case B to verify the mesh independence are shown in Figure 3.

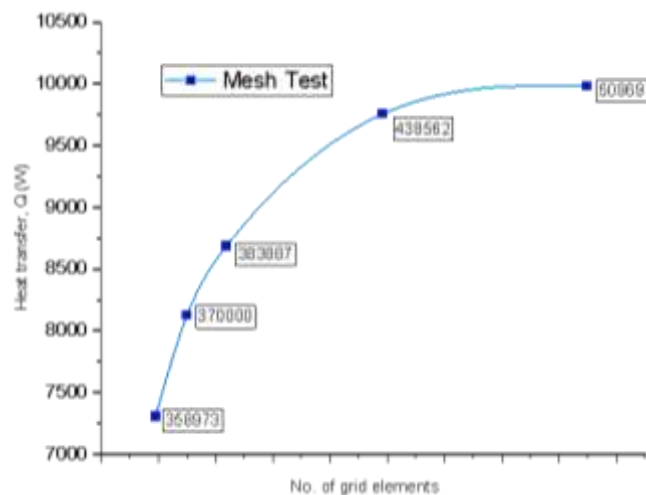


**Fig.3:-**Mesh independence test of the grid system for numerical solutions

## RESULTS AND DISCUSSION

To validate the numerical results of this study, tests of convective heat transfer coefficients,  $h$  (Eq. (12)) are performed for the cases A, B, C, and D. Moreover, these results have been compared with the results of Gunnasegaran et al. [15] Figure

4. The convective heat transfer coefficient in the shell side can be calculated by using the log mean temperature difference (LMTD) (Eq. (13)) method [4]. The convective heat transfer coefficient can be utilized to find out the area-weighted average Nusselt number using Eq. (17).

$$h = 0.36 \frac{K}{D_e} Re^{0.55} Pr^{0.33} \left( \frac{\mu_t}{\mu_w} \right)^{0.14} \quad (12)$$

$$LMTD = \frac{\Delta T_{max} - \Delta T_{min}}{\ln(\Delta T_{max}/\Delta T_{min})} \quad (13)$$

$$\Delta T_{max} = T_w - T_{in} \quad (14)$$

$$\Delta T_{min} = T_w - T_{out} \quad (15)$$

$$A_0 = N_t \cdot \pi d_0 L \quad (16)$$

$$Nu = 0.36 Re^{0.55} Pr^{0.33} \left( \frac{\mu_t}{\mu_w} \right)^{0.14} \quad (17)$$

The heat transfer rate in the shell side fluid is:

$$Q_{\dot{m}} = C_p \dot{m} (T_{out} - T_{in}) \quad (18)$$

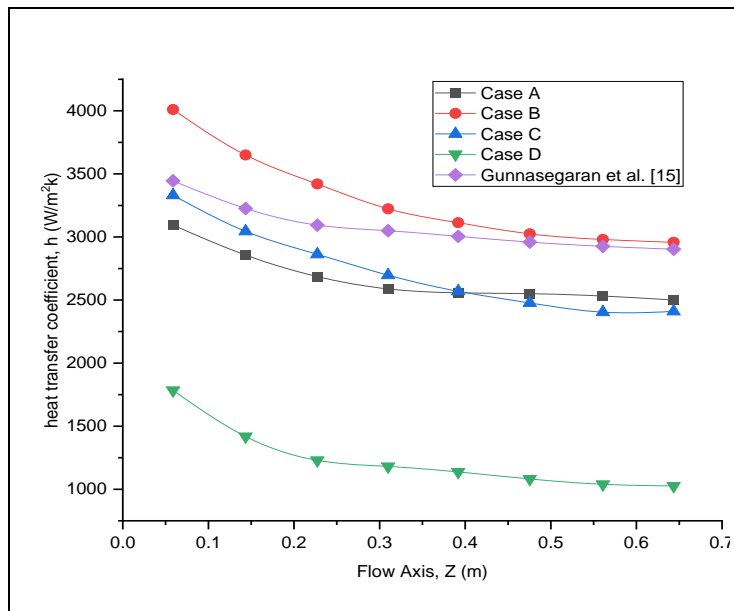




**Fig.4:-**Convective heat transfer coefficients along the flow axis for different baffle spaces (Case A, B, C & D)

The convective heat transfer coefficients are gradually decreasing in all cases with the flow along the tube lengths as shown in Figure 4. Similar results are also found by Gunnasegaran et al. [15] and by Dhamudia and Mishra [16].

It is seen that the baffle spacing has been playing a significant role in the effect of heat transfer coefficients. The heat transfer coefficient is increasing with the increase of baffle spacing. However, after

certain values of baffle spacing, the heat transfer coefficients are adversely affected by the larger baffle spacing. In this study, the least baffle spacing is 80 mm (Case A) and the highest is 150 mm (Case D).

In case B (100 mm baffle spacing), the heat transfer coefficients have been increased compared with case A. After case B, the heat transfer coefficients have been decreasing whether the baffle spacing has been increased.

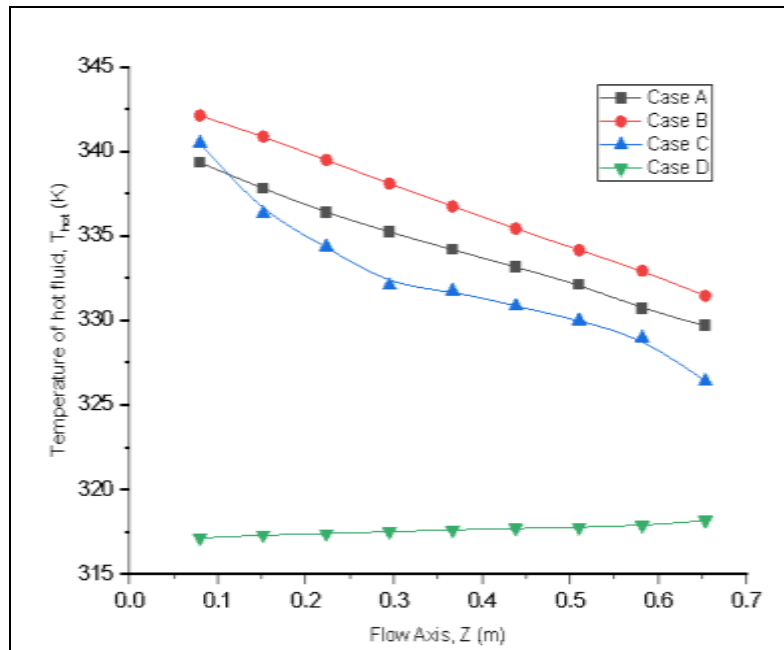


**Fig.5:-**Temperature variations of hot fluid along the tube length for different baffle spaces (Case A, B, C, D)

The variations of hot fluid temperature ( $T_{hot}$ ) along the flow axis for cases A, B, C, and D are depicted in Figure 5. It is obvious that the hot fluid temperature will decrease with the flow as a result of heat transfer to the cold fluid.

The more the heat transfer, the more the temperature differences of hot fluid between the inlet and outlet. It is seen in Figure 5 and 8, the temperature of hot

fluid decreases with the flow along the tube lengths.

For case B (baffle space 100 mm), the decreasing rate of hot fluid temperature is more uniform in comparison with the other cases.

In case A, the temperature decreasing rate would also be noticeable, however, due to the effects of turbulence and eddy viscosity (Figure 9 and 10) the

temperature variations become non-uniform. In case D, due to negligible turbulence and eddy viscosity, the temperature of the hot fluid remains almost constant i.e. there is no heat transfer occurs between hot fluid of tube and cold fluid of shell. The presence of turbulence has a strong influence on the heat transfer in STHX.

The more the turbulence present, the more the heat transfer will occur. Therefore, it

is desirable to design a system where the turbulence effect will generate at a significant amount. In Figure 6, it is seen that the turbulence effect has improved in case B and case C relative to case A. Whether in case D, the turbulence effect becomes too negligible to facilitate the heat transfer. Due to having larger baffle space in case D, the flow restrictions decrease along the flow axis as a result of which the turbulence effect has been reduced.

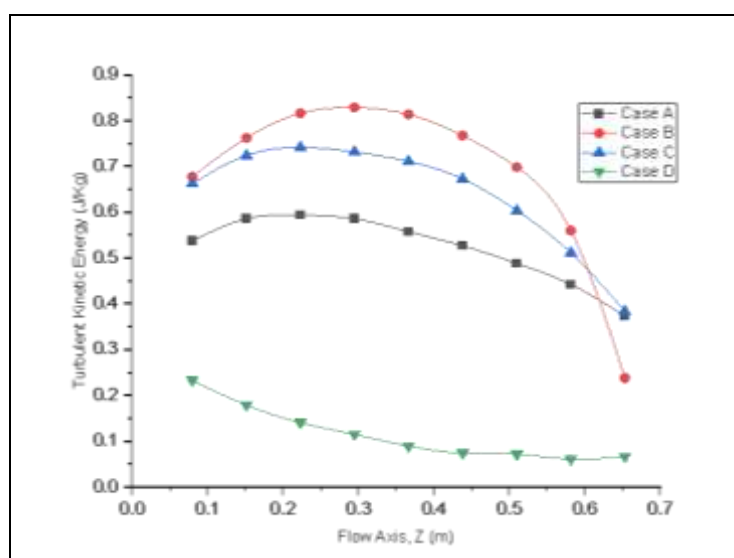


**Fig.6:-**The turbulent kinetic energy of hot fluid along flow axis for different baffle spaces (Case A, B, C, D)

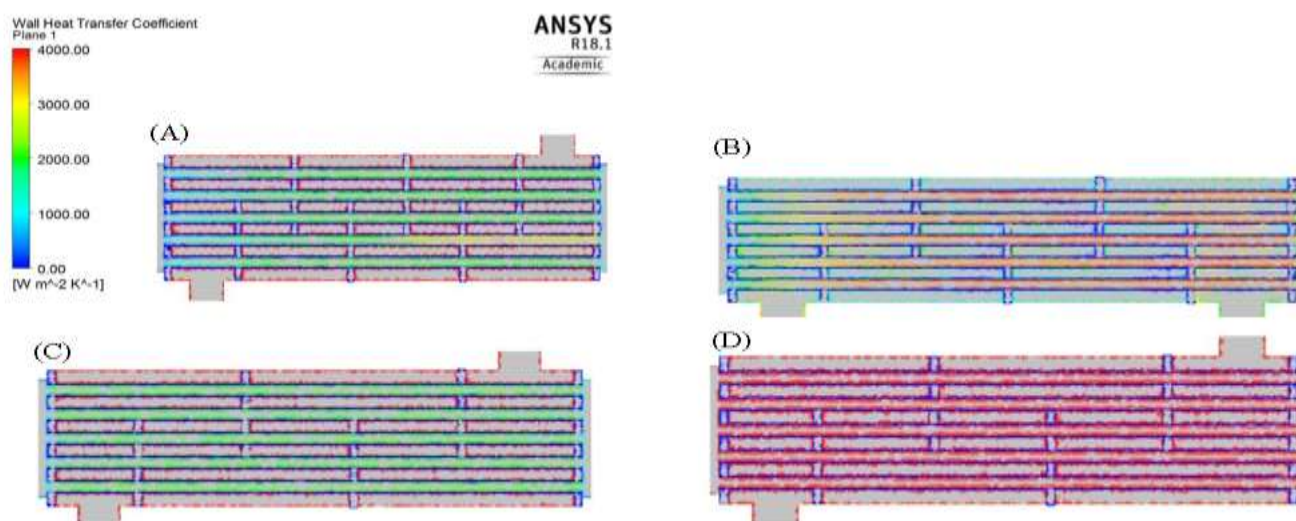


**Fig.7:-**Color map of wall heat transfer coefficients for the different baffle spaces and baffle numbers

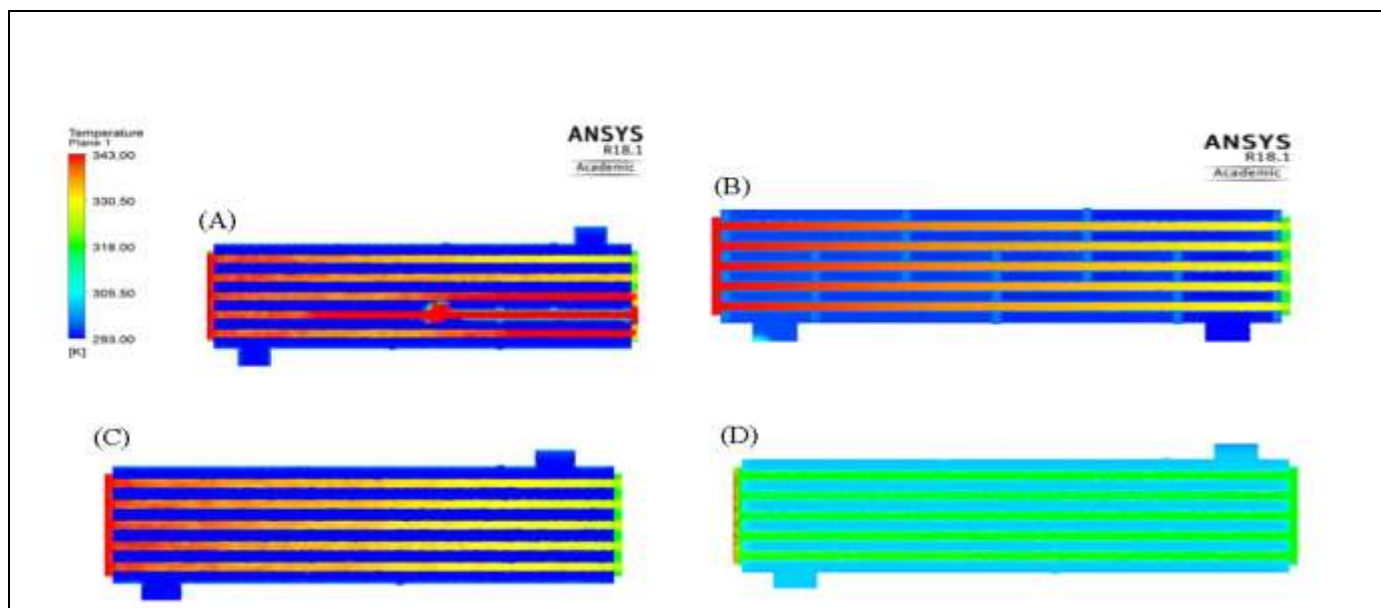


**Fig.8:-**Color map of temperature distributions for the different baffle spaces and baffle numbers

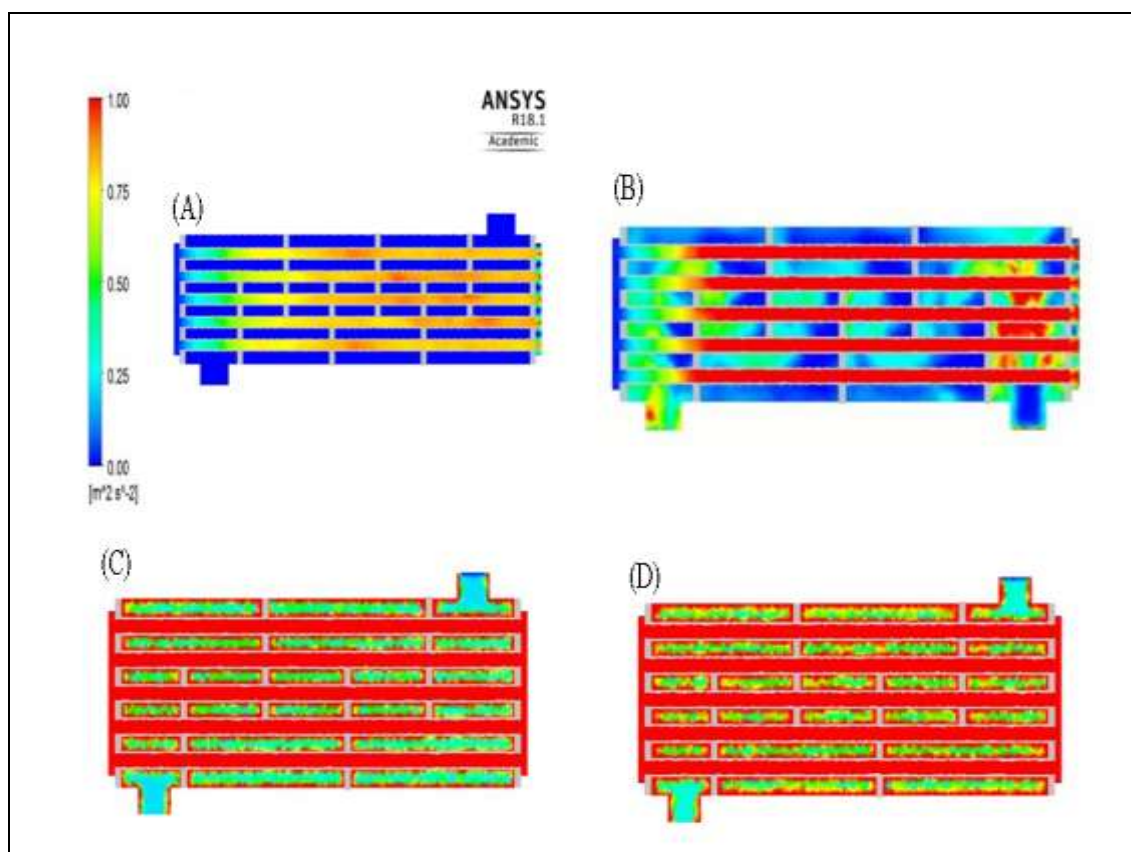


**Fig.9:-**Turbulent kinetic energy distributions for the different baffle spaces and baffle numbers

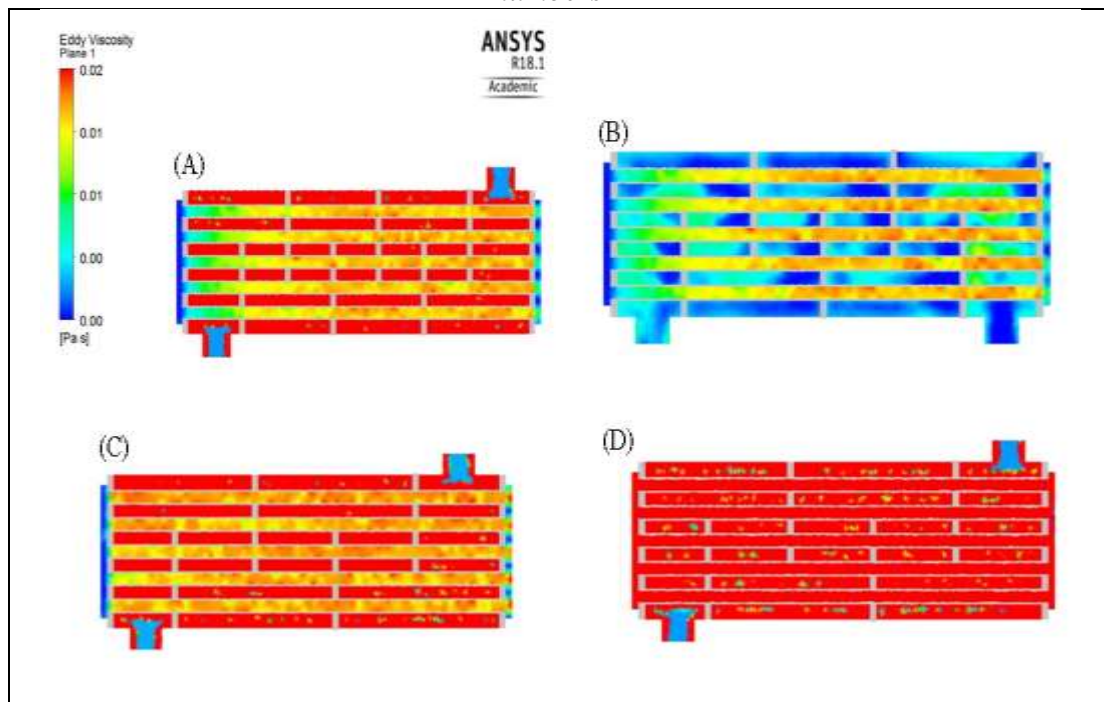


**Fig.10:-**Variations of eddy viscosity effects for the different baffle spaces and baffle numbers

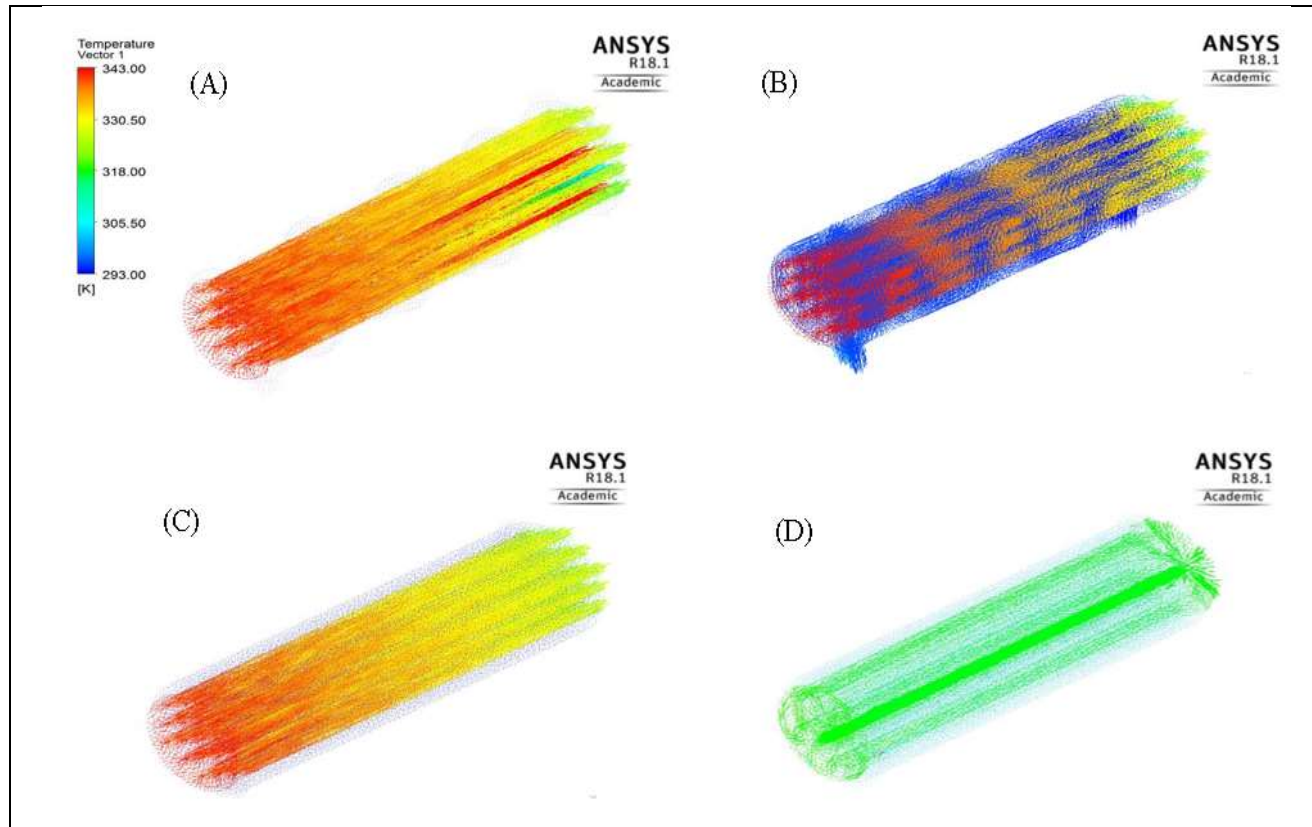


**Fig.11:-**Three-dimensional temperature distributions for the different baffle spaces and baffle numbers



*(In Figure 7- 11, (A), (B), (C) and (D) are indicating the case A, case B, case C, and case D, respectively)*

As discussed in the previous sections, baffle spacing and baffle numbers have a great influence on the thermal performance of an STHX. As shown in Figure 7, wall heat transfer coefficients are more uniform for cases A and B in comparison to cases C and D. Due to the effects of turbulence and eddy viscosity, the variation of heat transfer exists in a system of heat exchanging devices. The more the uniform distribution of turbulence intensity and the less the intensity of eddy viscous effects, the more the better heat transfer will occur.

The distribution of turbulence intensity as well as the distribution of eddy viscosity are strongly dependent on the appropriate baffle spaces and baffle numbers. In this study, the most uniformity in the turbulence intensity has been found in case B (100 mm baffle space with 5 baffle numbers) as being seen in Figure 9. Moreover, less intensity of viscous effects has been found in case B (Figure 10). The 3D temperature distribution also provides a similar significance as shown in Figure 11.

## CONCLUSIONS

In this research, numerical analysis of a 3D simulation by the commercial software ANSYS Fluent 18.1 of shell and tube heat exchanger has been conducted to study the effects of baffle spaces and baffle numbers on the significance of heat transfer rate and uniformity of temperature distributions. There are four different segmental baffle spacing in the shell and tube heat exchangers with the different number of baffles that have been conducted numerically. The simulations were conducted on a 600 mm long STHX with an inner diameter of 200 mm. A hexagonal arrangement of 19 tubes with an inner diameter of 20 mm and a thickness of 3 mm has been chosen. Due

to having good thermal conductivity, copper was selected as a construction material for both the shell and tube walls. The four different cases were simulated with the same boundary conditions at the inlets and outlets for the cold and hot fluids.

For the hot fluid in the tube, a mass flow rate of 2 kg/s with 343 K temperature at the inlet has been applied for all of the four different cases. For the cold fluid in the shell, a mass flow rate of 1.2 kg/s with 293 K temperature at the inlet has been applied for all the cases. Pressure outlets with gauge pressure as 0 pa were used at the outlets of the shell side and tube side fluids, simultaneously. Based on the results of our investigations, it can be summarized that the baffle spaces, baffle cut, and baffle numbers have significant impacts on the thermal performances of a segmental baffle STHX. The present study shows thermal performances of STHXs are adversely affected beyond a certain limit of baffle spaces and baffle numbers.

From the analysis of this research as described above, among the four different cases of segmental baffles, case B (100 mm baffle spaces with 5 baffles) shows the highest value of heat transfer coefficients and the most uniform distributions of turbulence and temperature variations. This research is largely convenient to elucidate that with an optimum value of baffle spaces can be designed to obtain a significant amount of heat transfer when it is coupled with a fewer number of baffles. It can be illustrated and recommended that an appropriate combination of baffle spaces and baffle numbers should prefer to acquire the most significant configuration.

## CONFLICTS OF INTEREST

The authors declare the confirmation of no conflict of interest related to this

research

work.

NOMENCLATURE	
$D_i$	Shell inner diameter [mm]
$t_s$	Shell thickness [mm]
$L$	Shell length [mm]
$d_i$	Tube inner diameter [mm]
$t_t$	Tube thickness [mm]
$B$	Baffle Space [mm]
$P_t$	Tube pitch [mm]
$C_p$	Specific heat [J/kg K]
$h_s$	Convective heat transfer coefficient [W/m <sup>2</sup> K]
$k$	Turbulent kinetic energy [J/kg]
$\dot{m}_{hot}$	Hot fluid mass flow rate [kg/s]
$\dot{m}_{cold}$	Cold fluid mass flow rate [kg/s]

$T_{hot}$	Hot fluid temperature [K]
$T_{cold}$	Cold fluid temperature [K]
LMTD	Log mean temperature difference [K]
$u$	Flow velocity
$Q$	Heat transfer rate [W]
$\dot{Q}$	Heat generation rate [W/m <sup>2</sup> ]
Nu	Nusselt number
$\mu_t$	Turbulent viscosity [Pa.s]
$\varepsilon$	Energy dissipation [m <sup>2</sup> /s <sup>3</sup> ]
$f$	Friction factor
$\eta$	Thermal enhancement factor
$\rho$	Fluid density [kg/m <sup>3</sup> ]

## REFERENCES

- Mellal, M., Benzeguir, R., Sahel, D., & Ameer, H. (2017). Hydro-thermal shell-side performance evaluation of a shell and tube heat exchanger under different baffle arrangement and orientation. *International Journal of Thermal Sciences*, 121, 138–149.
- Kern D. Q. (1950). Process heat transfer. New York: McGraw-Hill.
- Yehia, M. G., Attia, A. A. A., Abdelatif, O. E., & Khalil, E. E. (2016). Heat transfer and friction characteristics of shell and tube heat exchanger with multi inserted swirl vanes. *Applied Thermal Engineering*, 102, 1481–1491. <https://doi.org/10.1016/j.applthermaleng.2016.03.095>.
- Cengel Y. A. (1997). Introduction to thermodynamics and heat transfer. New York: McGraw-Hill.
- Wen, J., Yang, H., Wang, S., Xue, Y., & Tong, X. (2015). Experimental investigation on performance comparison for shell-and-tube heat exchangers with different baffles. *International Journal of Heat and Mass Transfer*, 84, 990–997. <https://doi.org/10.1016/j.ijheatmasstransfer.2014.12.071>.
- Ameer, H. (2020). Effect of corrugated baffles on the flow and thermal fields in a channel heat exchanger. *Journal of Applied and Computational Mechanics*, 6(2), 209–218. <https://doi.org/10.22055/jacm.2019.28936.1521>.
- Mohammadi, M. H., Abbasi, H. R., Yavarinasab, A., & Pourrahmani, H. (2020). Thermal optimization of shell and tube heat exchanger using porous baffles. *Applied Thermal Engineering*, 170(September 2019), 115005. <https://doi.org/10.1016/j.applthermaleng.2020.115005>.
- Gaikwad, S., & Parmar, A. (2021). Numerical simulation of the effect of baffle cut and baffle spacing on shell side heat exchanger performance using CFD. *Chemical Product and Process Modeling*, 16(2), 145–154. <https://doi.org/10.1515/cppm-2020-0033>.



9. Kumaresan, G., Santosh, R., Duraisamy, P., Venkatesan, R., & Kumar, N. S. (2018). Numerical Analysis of Baffle Cut on Shell Side Heat Exchanger Performance with Inclined Baffles. In *Heat Transfer Engineering* (Vol. 39, Issues 13–14). <https://doi.org/10.1080/01457632.2017.1363624>.
10. He, L., & Li, P. (2018). Numerical investigation on double tube-pass shell-and-tube heat exchangers with different baffle configurations. *Applied Thermal Engineering*, 143, 561–569. <https://doi.org/10.1016/j.applthermaleng.2018.07.098>.
11. Kayabasi, E., Alperen, M. A., & Kurt, H. (2019). The effects of component dimensions on heat transfer and pressure loss in shell and tube heat exchangers. *International Journal of Green Energy*, 16(2), 200–210. <https://doi.org/10.1080/15435075.2018.1555162>.
12. Abbasi, H. R., Sharifi Sedeh, E., Pourrahmani, H., & Mohammadi, M. H. (2020). Shape optimization of segmental porous baffles for enhanced thermo-hydraulic performance of shell-and-tube heat exchanger. *Applied Thermal Engineering*, 180, 115835. <https://doi.org/10.1016/j.applthermaleng.2020.115835>.
13. ANSYS Fluent Theory Guide, ANSYS, Inc. (August 2021) 2600 Ansys Drive Canonsburg, PA 15317, USA,
14. Nemati Taher, F., Zeyninejad Movassag, S., Razmi, K., & Tasouji Azar, R. (2012). Baffle space impact on the performance of helical baffle shell and tube heat exchangers. *Applied Thermal Engineering*, 44, 143–149. <https://doi.org/10.1016/j.applthermaleng.2012.03.042>.
15. Gunnasegaran, P., Shuaib, N. H., Abdul Jalal, M. F., & Sandhita, E. (2012). Application of nanofluids in heat transfer enhancement of compact heat exchanger. *AIP Conference Proceedings*, 1502(1), 408–425. <https://doi.org/10.1063/1.4769160>.
16. Dhamudia, K., & Mishra, P. K. (2021). Numerical investigation for improved heat transfer characteristics in micro-fin tubes. *Heat Transfer*, 50(1), 688–711. <https://doi.org/10.1002/htj.21899>.